

ADVANTAGES AND CHALLENGES OF Nb₃Sn SUPERCONDUCTING UNDULATORS*

A.V. Zlobin†, E. Barzi, D. Turrioni, Fermilab, 60510 Batavia, USA
 Yu. Ivanyushenkov, I. Kesgin, ANL, Argonne, Illinois

Abstract

Utilization of Nb₃Sn superconducting wires offers the possibility to increase undulators' nominal operation field and temperature margin, but requires overcoming challenges that are described in this paper. The achievable field levels for a Nb₃Sn version of superconducting undulators being developed at APS-ANL and the conductor choice are also presented and discussed.

INTRODUCTION

Due to the high critical current density, superconducting undulators (SCUs) outperform undulators based on permanent magnets in terms of the level of magnetic field. Most of the present SCUs, including devices built at the Advanced Photon Source (APS) of Argonne National Laboratory [1], use NbTi superconductor with a critical temperature $T_{c0}=9.8$ K and an upper critical magnetic field $B_{c20}=14.5$ T. Using Nb₃Sn superconductor, with critical parameters almost a factor of two higher than the NbTi parameters ($T_{c0}=18$ K and $B_{c20}=28$ T), offers the possibility of a substantial increase of both the SCU operation fields and its temperature margin.

Since the end of the 1990s, the critical current density J_c at high fields in modern commercial Nb₃Sn composite wires has made impressive progress [2], mainly driven by the needs of high field magnets for accelerators. SCUs can benefit from the high J_c of Nb₃Sn wires too, as long as conductor stability can be provided. Stability to flux jumps in superconductor is a critical issue for high- J_c Nb₃Sn wires. This problem was actively discussed and practically resolved for Nb₃Sn wires used in high field magnets [3]. For SCU applications it is still current, due to the low operation fields and high current density in the conductor.

Tests of the first Nb₃Sn SCU models suffered from long training and large critical current degradation, which were attributed to flux-jump instabilities and epoxy cracking in the Nb₃Sn coils [4-8]. Based on the progress of Nb₃Sn composite wires and of the Nb₃Sn accelerator magnet technology, work on Nb₃Sn SCUs was resumed at ANL in collaboration with FNAL. The possibilities and limitations of Nb₃Sn SCU models are discussed in this paper.

SCU DESIGNS

The magnetic field in a planar SC undulator is generated by two identical windings separated by a gap for the

beam pipe. Each winding consists of a series of vertical racetrack coils which are powered in opposite directions and are separated by magnetic poles. The conceptual design of the SCUs developed at ANL, and the SCU coil cross-section scheme are shown in Figs. 1 and 2.

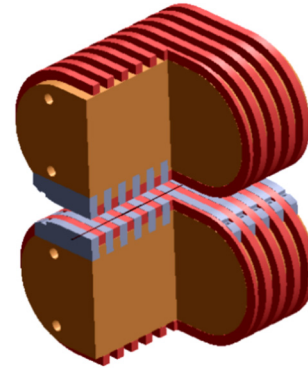


Figure 1: ANL SCU section 3D view.

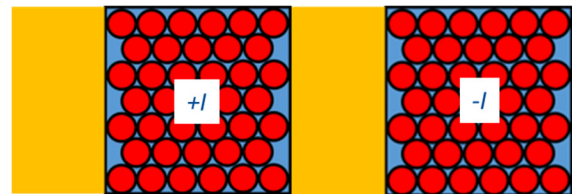


Figure 2: ANL SCU coil cross-section scheme.

Table 1: NbTi and Nb₃Sn SCU Parameters

	Reference design	Design 1	Design 2
Pole width, mm	3.65	3.05	3.65
Coil width, mm	4.6	5.2	4.6
Coil thickness, mm	4.85	5.5	4.8
Superconductor	NbTi	Nb ₃ Sn	Nb ₃ Sn
Wire diameter, mm	0.7	0.7	0.6
Insulation thickness, mm	0.025	0.075	0.075
Insulated wire diameter, mm	0.753	0.85	0.75

Geometrical and conductor parameters for the reference NbTi SCU and for the Nb₃Sn SCU R&D models (Design 1 and Design 2) are summarized in Table 1. All the SCUs have the same period of 16.5 mm and 39 turns per coil, and a magnetic gap of 8 mm. Each coil has rectangular cross-section and is wound using round insulated wire. The NbTi wire is insulated with 0.025 mm thick Formvar insulation, whereas the Nb₃Sn wires are insulated with 0.075 mm thick S2-glass sleeve. Each coil has 7 conductor layers with 6 turns in the even layers and 5 turns in the odd layers (see Fig. 2). This scheme provides compact coil winding, but has 6 voids with relatively large areas. Filled with epoxy, they may substantially impact the magnet quench performance due to epoxy cracking at low temperatures under large Lorentz forces.

* Work is supported by Fermi Research Alliance, LLC, under contract No. DE-AC02-07CH11359 with the U.S. Department of Energy and by the U.S. Department of Energy, Office of Science, Office of Basic Energy Sciences, under Contract No. DE-AC02-06CH11357.

†zlobin@fnal.gov

EFFECT OF SCU DESIGN AND SUPER-CONDUCTOR PARAMETERS

Figure 3 shows the critical current vs. magnetic field of a typical 0.7 mm NbTi wire with $J_c(5T,4.2K)=2.5$ kA/mm² and of a 0.6 mm Nb₃Sn wire with $J_c(12T,4.2K)=2.5$ kA/mm², averaged over the total coil cross-section of the reference NbTi and the Design 2 Nb₃Sn SCUs. The corresponding SCU load lines for the maximum field in the coil B_c, and for the maximum field in the SCU aperture B_a are also shown. Due to the similar coil cross-section parameters, the corresponding load lines are practically identical for both SCU designs.

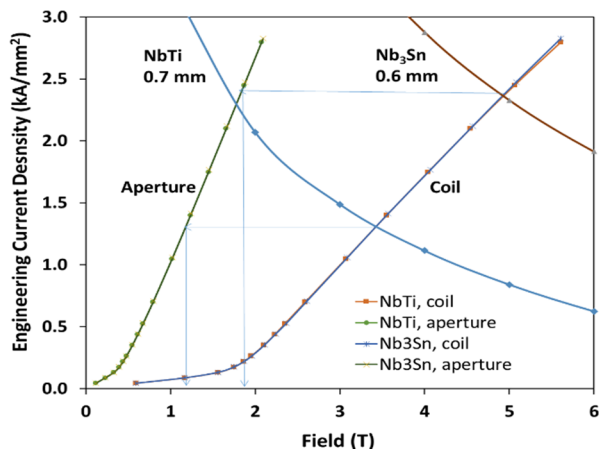


Figure 3: Comparison of maximum coil B_c and aperture B_a fields of Nb₃Sn (Design 2) and NbTi SCUs.

The data in Fig. 3 show that in the Nb₃Sn SCU the coil maximum field B_c is ~5 T, and the maximum aperture field B_a is 1.8 T, whereas in the NbTi SCU these values are limited at 3.5 T and 1.2 T respectively. Thus, using Nb₃Sn conductor allows increasing the SCU performance by 50%. However, the current density in Nb₃Sn SCUs reaches rather high values of ~10 kA/mm², whereas in NbTi SCUs it is only ~4 kA/mm², i.e. 2.5 times smaller. Such high J_c in Nb₃Sn SCU may lead to flux-jump stabilities and magnet protection issues.

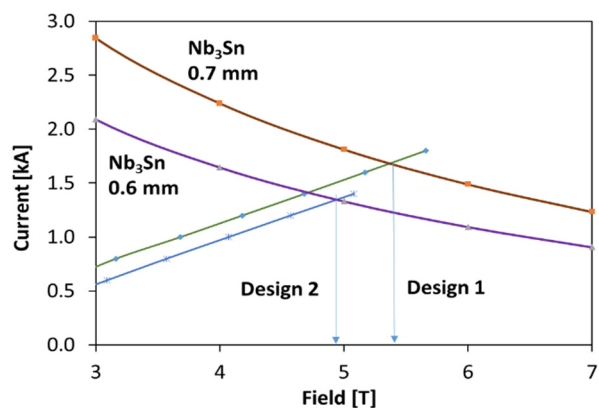


Figure 4: Load lines and conductor I_c(B) curves for Nb₃Sn Design 1 and Design 2 SCUs.

Figure 4 compares the efficiency of Nb₃Sn SCU Design 1 and Design 2. One can see that Design 1, based on 0.7

mm wire, reaches a maximum coil field and a maximum aperture field that are 10% higher than in Design 2.

Figure 5 shows the sensitivity of the maximum fields in the coil B_c and in the aperture B_a with respect to the conductor J_c at 12 T and 4.2 K for the Nb₃Sn SCU (Design 2). A B_c>5 T in this design can be achieved with Nb₃Sn wires having a quite high J_c(12T,4.2K) of 2.8 kA/mm² if conductor stability to flux jumps is provided. One can also see that increasing the conductor J_c from 2 to 3 kA/mm² (i.e. by 50%) changes B_c and B_a only by ~20%. Thus, since flux-jump instabilities are proportional to the conductor J_c, its optimization can be used to reduce the performance degradation of Nb₃Sn coils due to this effect.

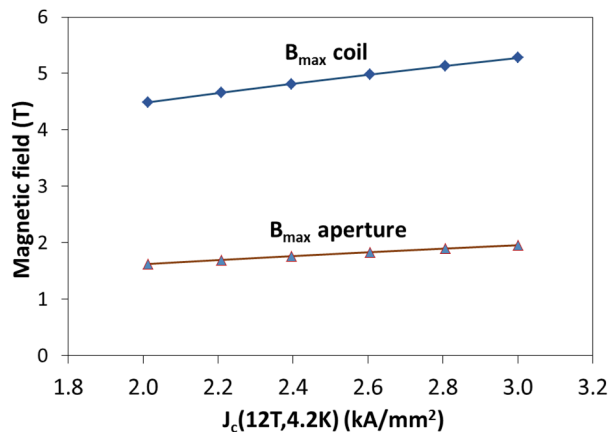


Figure 5: Maximum field B_c in coil and maximum field B_a in aperture vs. conductor critical current density J_c(12T,4.2K) for Nb₃Sn (Design 2) SCU.

STUDY OF Nb₃Sn WIRES FOR SCUs

According to the adiabatic stability model [3], to be stable at the coil maximum design field of ~5 T, the product of the conductor J_c(12T,4.2K) by the subelement (SE) diameter D_S has to be less than 120 A/mm. The maximum D_S vs the conductor J_c(12T, 4.2K) required to provide stable SCU performance for a maximum coil field of 5 T is shown in Fig. 6. Thus, Nb₃Sn wires with D_S less than 40 μm are stable at J_c(12T,4.2K) values up to 3 kA/mm².

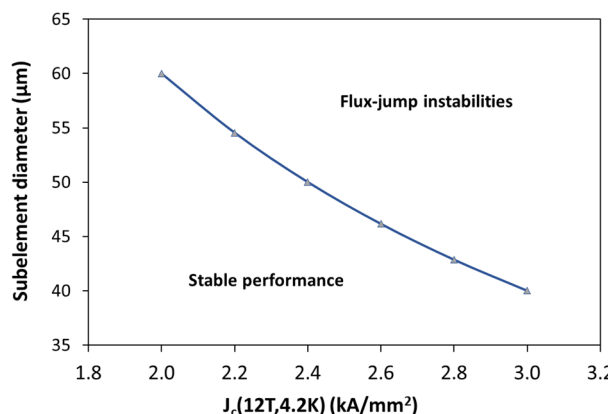


Figure 6: Maximum D_S vs. conductor J_c(12T,4.2K).

Several Nb₃Sn RRP wires produced by Bruker-OST were examined for use in the ANL-FNAL SCU models.

Parameters of the Nb₃Sn wires are summarized in Table 2. The wire cross-sections are shown in Fig. 7. Wires of same architecture have the same average SE size, but slightly different number of subelements and their distribution inside the wire cross-section and, thus, different fraction of Cu. Measurements of the SE size distribution in the wire cross-section have shown a $\pm 20\%$ spread with respect the nominal numbers presented in Table 2.

Table 2: Nb₃Sn Wire Parameters

	RRP127	RRP169	
Wire diameter, mm	0.7	0.7	0.6
Number of SEs	108, 114	150	132, 150
SE diameter, μm	41	36	31
Cu fraction, %	54, 52	52	56, 50

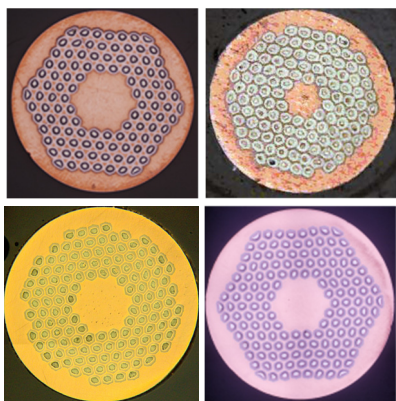


Figure 7: Cross-sections of RRP108/127 and RRP114/127 (top), and RRP132/169 and RRP150/169 (bottom) Nb₃Sn composite wires.

Figure 8 shows the critical current vs. field measured for 0.7 mm diameter RRP114/127 and RRP150/169 wires, and the SCU Design 1 load line. Both wires have $J_c(12\text{T}, 4.2\text{K}) = 2.65 \text{ kA/mm}^2$ and a RRR of 58 and 117 respectively. The theoretical $I_c(B)$ dependence was calculated using a parameterization which fits the experimental data at high fields, where the wires show smooth transition from superconducting to normal state.

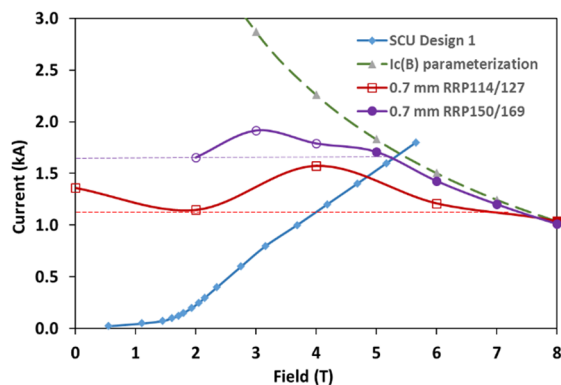


Figure 8: Critical current vs. field for 0.7 mm diameter RRP114/127 and RRP150/169 wires and the SCU Design 1 load line. Closed markers represent I_c values, whereas open markers indicate premature quenches.

For the RRP114/127 wire, stable transition was measured at fields above 8 T. At lower fields the samples quenched prematurely. The minimum quench current for this wire at low fields was $\sim 1.1 \text{ kA}$. For the RRP150/169 wire with smaller SE size, stable performance was measured down to 5 T. At lower fields, the conductor current was limited at 1.65 kA due to flux-jump instabilities. These data are consistent with the theoretical predictions in Fig. 6. Based on the data in Fig. 8, to achieve the conductor limit in the SCU Design 1, an RRP169 or wire with SE size smaller than $36 \mu\text{m}$ has to be used.

Sensitivity to flux jumps can be also partially reduced by increasing the matrix residual resistivity ratio (RRR) for conductor dynamic stabilization. Appropriate optimization of the heat treatment (HT) cycle can provide significant increases in RRR with an acceptable decrease in conductor critical current density. Figure 9 shows the dependence of $J_c(12\text{T}, 4.2\text{K})$ and wire RRR vs. maximum reaction temperature for a duration of 50 hrs. Wire reaction at

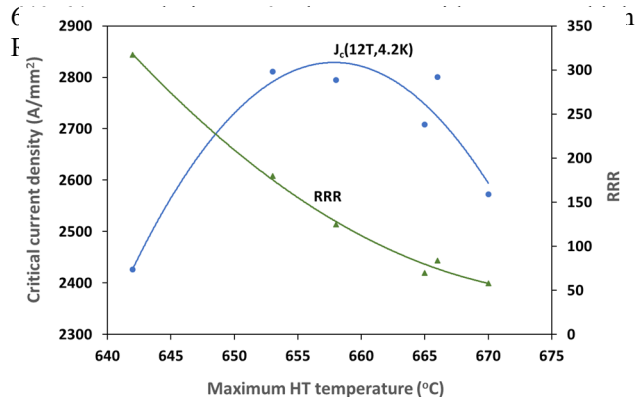


Figure 9: Wire $J_c(12\text{T}, 4.2\text{K})$ and RRR vs. maximum reaction temperature during 50 hours.

CONCLUSION

Analysis shows that the Nb₃Sn SCUs being developed by the ANL-FNAL collaboration can reach a maximum field in the coil of $\sim 5 \text{ T}$ (Design 2) and of $\sim 5.5 \text{ T}$ (Design 1). To achieve this performance, wires with $J_c(12\text{T}, 4.2\text{K}) > 2.8 \text{ kA/mm}^2$ are needed. The high J_c in the coil requires serious attention to conductor stability with respect to flux jumps. Particularly, the transverse size D_S of the superconducting subelements has to be $36 \mu\text{m}$ or less. Performed experimental studies of several Nb₃Sn RRP wires produced by Bruker-OST confirmed that the required stability at the expected fields and currents can be achieved by using RRP169 wires with diameter of 0.7 mm or less. Optimization of the RRP wire HT provides additional possibilities to improve conductor stability by controlling J_c and matrix RRR.

REFERENCES

- [1] Y. Ivanyushenkov, "Magnetic simulation of a superconducting undulator for the advanced photon

- source,” *Proc. of PAC2009*, Vancouver, Canada, 2009, p. 310.
- [2] E. Barzi and A.V. Zlobin, “Research and Development of Nb₃Sn Wires and Cables for High-Field Accelerator Magnets,” *IEEE Trans. on Nuclear Science*, vol. 63 (2), 2016, p. 783.
- [3] A.V. Zlobin, V.V. Kashikhin, and E. Barzi, “Effect of magnetic instabilities in superconductor on Nb₃Sn accelerator magnet performance,” *IEEE Trans. Appl. Supercond.*, vol. 16 (2), 2006, p. 1308.
- [4] S.O. Prestemon *et al.*, “Design, Fabrication, and Test Results of Undulators Using Nb₃Sn Superconductor,” *IEEE Trans. on Appl. Supercond.*, vol. 15 (2), 2005, p. 1236.
- [5] S.H. Kim *et al.*, “R&D of short period Nb-Ti and Nb₃Sn superconducting undulators for the APS,” *Proc. PAC05*, 2005, p. 2419.
- [6] H.W. Weijers *et al.*, “A Short-Period High-Field Nb₃Sn Undulator Study,” *IEEE Trans. on Appl. Supercond.*, vol. 16 (2), 2006, p. 311.
- [7] D.R. Dietderich *et al.*, “Fabrication of a Short-Period Nb₃Sn Superconducting Undulator,” *IEEE Trans. on Appl. Supercond.*, vol. 17 (2), 2007, p. 1243.
- [8] H.W. Weijers *et al.*, “Assembly Procedures for a Nb₃Sn Undulator Demonstration Magnet,” *IEEE Trans. on Appl. Supercond.*, vol. 17 (2), 2007, p. 1239.